N79-17493

DRIVER STEERING DYNAMICS MEASURED IN A CAR SIMULATOR UNDER A RANGE OF VISIBILITY AND ROADMARKING CONDITIONS

R. Wade Allen and Duane T. McRuer
Systems Technology, Inc.
Hawthorne, California

Abstract

A simulation experiment was conducted to determine the effect of reduced visibility on driver lateral (steering) control. The simulator included a real car cab and a single lane road image projected on a screen six feet in front of the driver. Simulated equations of motion controlled apparent car lane position in response to driver steering actions, wind gusts, and road curvature. Six drivers experienced a range of visibility conditions at various speeds with assorted roadmarking configurations (mark and gap lengths).

Driver describing functions were measured and detailed parametric model fits were determined. A pursuit model employing a road curvature feedforward was very effective in explaining driver behavior in following randomly curving roads. Sampled-data concepts were also effective in explaining the combined effects of reduced visibility and intermittent road markings on the driver's dynamic time delay. The results indicate the relative importance of various perceptual variables as the visual input to the driver's steering control process is changed.

INTRODUCTION

Automobile steering control is a dynamic task that is performed by the driver in order to establish and/or maintain the vehicle on a specified pathway in the presence of inputs such as crosswinds and roadway curvature. The motions of an automobile in response to steering actions and aerodynamic disturbances can be described in terms of differential equations, transfer functions, etc. (Ref. 1), and it is logical to attempt to describe the driver in similar terms.

In the research described herein the motivation for a dynamic description and measurement of the driver was twofold: 1) to determine and quantify the effect of adverse visibility on driver perception of the cues required for steering control; and 2) to determine those changes in driver behavior that contribute to degraded performance under conditions of reduced visibility. An understanding of these effects may then suggest countermeasures to vehicle control problems associated with adverse visibility.

PERCEPTION AND DRIVER/VEHICLE SYSTEM GUIDANCE REQUIREMENTS

Given that road delineation features (e.g., dashed lines) are detected, the driver's perceptual processes can then extract information for vehicle control. Adverse visibility conditions can reduce visual range (Ref. 2), and the question to be considered here is how reduced visibility might affect driver perception of vehicle path and subsequent control actions.

An abstraction of the driver's perceptual task is illustrated in Fig. 1, a perspective view of a single lane bounded by dashed lines. With forward motion in a straight line the driver's visual scene appears to expand from a perspective vanishing point at infinity. Theories have been advanced for a focus or center of expansion perception of motion (Ref. 3). On straight roads the center of expansion is the only point in the visual field that is apparently stationary, and it would provide a direct cue for the car's path angle. Thus, when forward view is reduced by adverse visibility, direct perception of path angle is denied the driver according to the focus of expansion theory. This theory has some problems, however. As Gordon (Ref. 4) notes, for curved paths the center of expansion lies at the center of curvature, which is at right angles to the path of the vehicle. Furthermore, Palmer (Ref. 5)

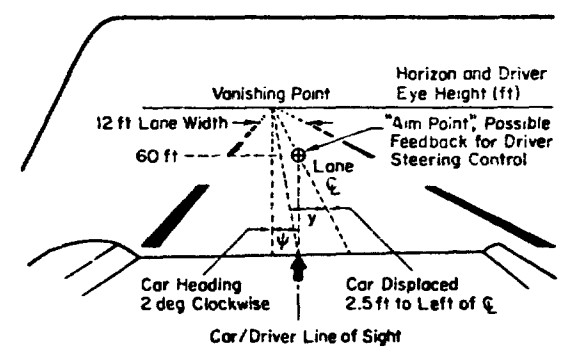

Figure 1. Driver's Perspective View of a Single Delineated Path Illustrating an Aim Point Control Law

has found that the center of expansion in visual fields expanding at various constant rates of expansion can only be perceived within 1-6 degrees of visual angle, which is much too coarse for vehicular control.

In a perspective motion field the streamers themselves play a more important role in the views of Calvert (Ref. 6), who emphasized their role in both directional and longitudinal control of aircraft on the final approach, and Gordon (Ref. 4), who considered terrestrial vehicles. The streamer theory states in essence that the driver perceives motion from objects in the visual field streaming across his field of view. Although the streamers emanate from the center of expansion, Gordon believes that it is the streamers themselves, particularly those provided by roadway boundaries and lane markings, that underlie the directional cue rather than the center of expansion. He notes that all parts of the visual field, road borders, and lane markers move when the wheel is turned but no one part is essential for tracking, and that the driver responds to a total situation (a Gestalt concept), not to isolated or ranked cues. Streamer perception should be fairly robust in the face of reduced visibility, although adverse visibility (i.e., rain, fog) would eliminate many subtle cues (e.g., road roughness, edge texture), particularly those available outside foveal vision where contrast sensitivity and acuity degrade (Ref. 7).

Control theory analysis and research into land vehicle steering control have identified cues that must be perceived either explicitly or implicitly in order to give good, stable performance. The car's position relative to the delineated path is the most obvious of these. Various studies have also demonstrated that heading or path angle is essential to achieving stable control (as reviewed in Ref. 8). Thus, properly weighted components proportional to lateral position and heading must be present in the driver's steering wheel deflection if the car's path is to be regulated in the lane.

One intuitively appealing model for driver lateral control involves steering inputs based on an aim point down the road as illustrated in Fig. 1. The aim point angle is one way to combine lateral position and preview-range-weighted heading into a single control quantity. The dynamics of this simple control model, among others, have been analyzed previously (Ref. 9). For an

aim point at a distance, x_a, a look-ahead or preview time constant dependent on vehicle speed, U_o, can be defined as follows:

$$T_a = \frac{x_a}{U_o} \qquad (1)$$

McLean (Ref. 10) has reviewed a number of driving experiments involving variations in restricted forward view and vehicle speed which found preview times (T_a) of 2 sec or greater. The results were quite variable, however, and it would be difficult to decide on an average or typical preview time constant.

If there is a preferred look-ahead distance or time constant, then restricted visual range due to adverse visibility could interfere with this cue, and visual ranges shorter than the preferred look-ahead distance would be expected to deteriorate performance. Lane position and heading cues do not necessarily have to be perceived at a combined aim point, however. Referring again to Fig. 1, simple geometric analysis shows that for small angles the car's heading angle deviations with respect to the lane appear as horizontal translations of the visual scene. For car lateral position deviations with respect to the lane the road appears to rotate about its vanishing point at the horizon. Thus heading and lateral positions are separately available from the perspective view <u>if</u> a sufficient segment of this view is visible.

DRIVER/VEHICLE SYSTEM DYNAMIC MODEL

To gain further insight into driver perceptual requirements, consider the detailed driver/vehicle system dynamic model illustrated in Fig. 2. Here the vehicle model gives heading angle and lateral lane deviations (ψ and y) in response to driver steering commands (δ_w). The driver develops steering commands based on his perception of lane position and heading angle errors, plus an additional term proportional to perceived road curvature. The y and ψ perceptions are basically involved in regulation-only driver control, which is handled in a compensatory fashion. The added curvature term is a pursuit or feedforward element needed to account for driver behavior on curved roads. It basically assumes the driver inserts an open-loop steering wheel command

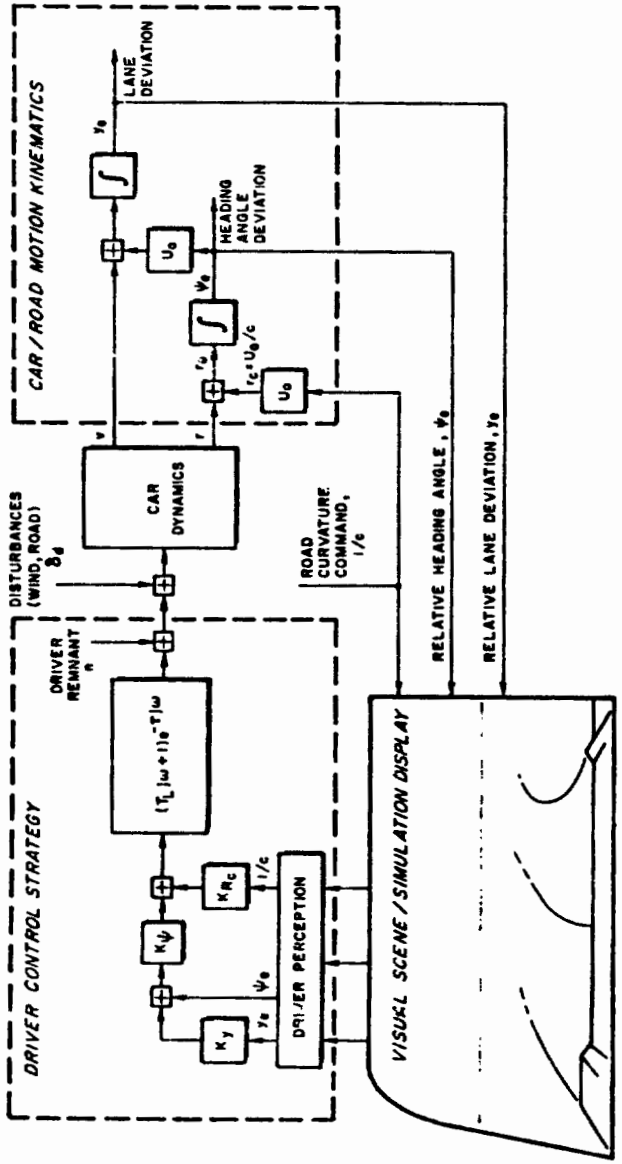

Figure 2. A Driver/Vehicle Dynamic System Model for Analyzing Adverse Visibility Effects on Steering Control

proportional to perceived path curvature. Some anticipation or driver lead (T_L) is applied to these perceptions to offset vehicle lag, and a time delay penalty (τ) is incurred by the driver due to basic neuromuscular characteristics and perceptual processing load. A final component of the driver's steering action is composed of remnant which is basically noise or random variation in the driver's output uncorrelated with perceptual inputs.

The regulation or error correcting portion of the Fig. 2 model, involving only lane position and heading error feedbacks (y_e and ψ_e, respectively) has been shown to have good, stable control properties (Ref. 11) and to be consistent with experimental measurements (Refs. 9 and 12). This mode of control is termed compensatory in that the driver is "compensating" for disturbance caused errors. In the case of a wind disturbance the driver has no perception or preview of the disturbance, and must wait for the disturbance to affect the vehicle's motion before responding.

When following a curving road (a path command) with sufficient visual range, the driver has the opportunity to preview or anticipate the desired path. With a visual segment large enough to permit adequate perception of the road's curvature, the driver can achieve a pursuit mode of control behavior and very nearly duplicate the commanded path. This is simply accomplished by the driver because in steady state the curved path followed by a car is nearly directly proportional to front wheel angle (Ref. 13), and the vehicle lags are well-learned and can be anticipated. Thus, the driver merely steers with actions directly proportional to perceived road curvature, sufficiently advanced in time to offset vehicle lag. Disruption of the curvature cue will degrade pursuit performance, however, which is a possibility with various combinations of adverse visibility and delineation as discussed previously.

COMPENSATORY VERSUS PURSUIT BEHAVIOR

Consider now the control and performance implications of compensatory and pursuit behavior. Given the model structure of Fig. 2 and nominal driver parameters obtained in this study under good visibility at 30 mph, we have analyzed the dynamic implications of curvature perception. Referring to Fig. 2, consider the driver/vehicle system response due to a command path

input. The commanded path causes an equivalent heading rate input, r_c, to be applied to the system. Driver steering action should then create vehicle yaw rates, r, which are nearly equal to the commanded heading rate so as to give a small heading rate error, r_e, which is the difference between the command input and the vehicle's motion.

To illustrate the potential improvement in performance between pursuit and compensatory driving we can consider the describing function relating heading rate error, r_e, to heading rate input command, r_c. Figure 3 shows Bode plots of this driver/vehicle system ratio as the curvature perception parameter (driver's "pursuit gain"), K_{R_C}, is increased. The compensatory baseline curve ($K_{R_C} = 0$) is based on a representative set of driver/vehicle data, and the other curves simply indicate the effect of $|r_e/r_c|$ when the additional driver control pathway represented by K_{R_C} is added. At low frequencies the describing function amplitude shows that errors are less than the original input, while at very high frequencies they may be somewhat greater. Note in particular that for the ideal no-lag vehicle an optimum

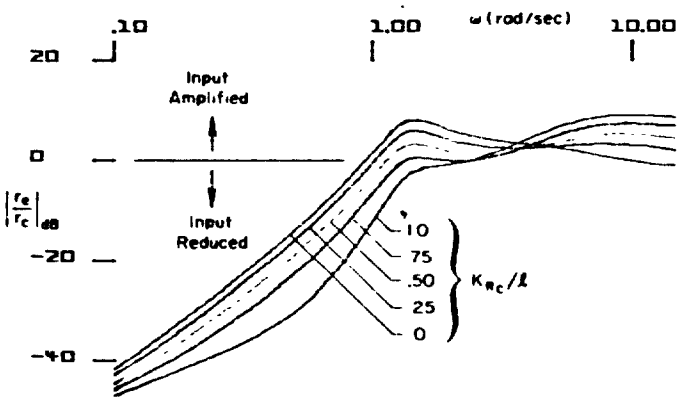

Figure 3. Effects of Variations in the Curvature Perception Gain on the Heading Error Rate to Heading Rate Input Transfer Function

value* of $K_{R_C}/\ell = 1$, errors in the frequency region of 0.3-1.0 rad/sec give a reduction in error of about 15 dB or a factor of greater than 5 times! At any given frequency, lane dispersions are directly proportional to heading rate errors and thus the curvature perception in the above frequency region would reduce lane dispersions by more than a factor of 5.

ADVERSE VISIBILITY EFFECTS

The Fig. 2 model can serve as the basis for some observations about driver visual perception requirements and potential effects of degraded visibility. Consider first the driver's use of the aim point concept illustrated in Fig. 1. Here reductions in visual range under adverse visibility conditions can eliminate the cues required to directly perceive the aim point. In this case the driver can extrapolate from the available cues or, alternatively, separately perceive lateral and heading error deviations. In either case, however, the driver is faced with an increased perceptual load. Past research has shown that increased perceptual load leads to increases in time delay (τ) and noise or remnant (Refs. 14 and 15). These effects should increase with decreased visual range.

When reduced visual range interferes with direct perception of the aim point, the lane delineation configuration then should become an important factor. Consider Fig. 1 with restricted preview. The driver needs adequate information to perceive ψ_e, y_e, and road curvature. If several delineation elements are visible, or single elements are of sufficient length, these variables should be directly perceivable. If element length is reduced, however, so that path direction is not readily indicated by a single element, then two components are needed to define direction and three to indicate curvature. In terms of the Fig. 2 model, a visual segment which contains at least three elements is needed for development of the K_{R_C} feedforward, while at least two elements are needed for ψ_e to be estimated. Thus the driver/vehicle system dynamics will depend strongly on the dimensions of the visual segment. As

*For the essentially neutral steer car of this study the steady-state turn radius is equal to the wheelbase divided by the front wheel angle (Ref. 13), so the curvature perception gain should be equal to the car's wheelbase, in this case 9.25 feet.

it is reduced, performance on curves will be degraded first (K_{R_C} reduced), followed by deterioration in lane position control. For segmented delineation the driver's input information also becomes perceptually intermittent as the visual segment is reduced, and intermittency has been shown to lead to increased time delay and remnant in the human operator (Ref. 15).

Besides providing insight into degraded visibility effects, the Fig. 2 model also serves as a paradigm for data measurement and analysis. The driver control strategy parameters in Fig. 2 can be determined through Fourier analysis techniques (Ref. 9) during driving tests involving regulation against disturbances, and following winding roads. This technique was used here as described further on to measure the perceptual/behavioral effects of adverse visibility, simultaneously during a single realistic task (in situ as it were), rather than requiring a series of artificial tests to isolate each effect.

EXPERIMENTAL METHODS

Simulation Setup

A fixed-base driving simulator was used to test the concept discussed previously. The physical arrangement of the simulator is illustrated in Fig. 4. Simulator details have been described previously (Ref. 16). The simulator had a high quality, wide angle video projection display of roadway markings as illustrated. Display perspective and motion were correctly represented with respect to the driver's eye position, and the electronic display generator was designed to allow a variety of delineation configurations and visibility conditions. Apparent road motion relative to the cab was controlled by driver steering, acceleration, and braking actions through equations of motion mechanized on an analog computer.

Delineation configuration and visual range could easily be controlled from an experimenter's console. The mark and cycle lengths of dashed delineation lines could be independently selected in discrete steps. The range extent of the visual segment could be set continuously from zero to a maximum display generator range of 300 ft. Visual range was controlled by an electronic intensity function which smoothly decreased display delineation line luminance as

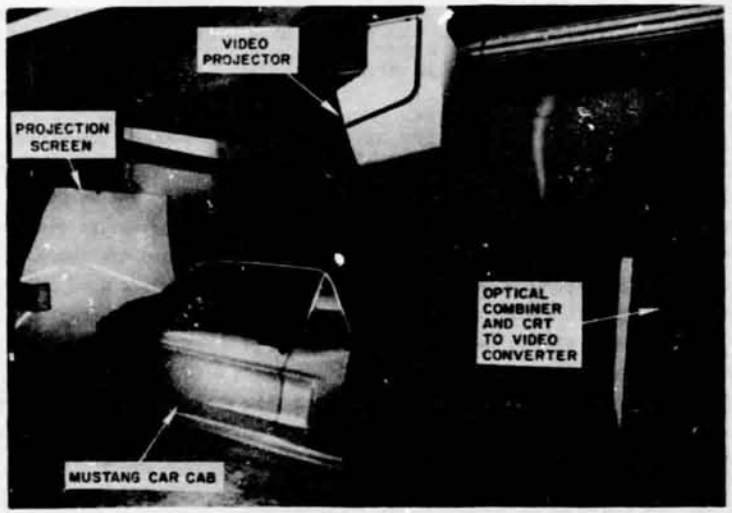

Figure 4. Driving Simulator Physical Arrangement

a function of distance down the road. Desired visual range was set subjectively as described later. This gave the desired physical results directly and minimized the need to control or account for all the subtle photometric and subjective effects which determine threshold contrast.

Experimental Design

Based on an exploratory series of tests the test matrix shown in Fig. was evolved. The matrix includes the important range of the three major variables of interest: visibility range, delineation configuration, and speed. The visibility range extends from close to the minimum possible for steering control (35 ft) out to a distance beyond that required for good control. Speed variations are covered from very slow to the current nationwide speed limit. Delineation configuration applies to a single lane delineated with left and right boundaries and covers a California standard with

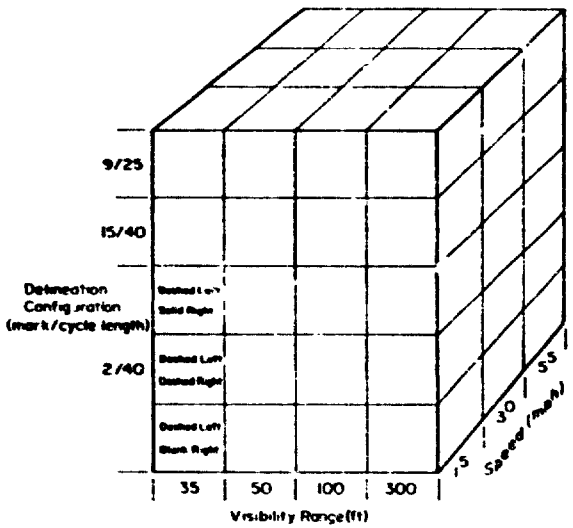

Figure 5. Simulator Test Condition Matrix

9 ft marks and 25 ft cycle (Ref. 17), the national standard recommendations of 15 ft marks and 40 ft cycles (Ref. 18), and a very short element spaced at 40 ft meant to simulate retroreflectors which individually offer no directional cues. A further variation was applied to the right boundary of the retroreflector delineation which included either a solid, dot (reflector) or blank (no right edge line) configuration. A solid edge line would presumably improve performance over that with dotted elements, while the lack of any edge line at all would degrade performance under adverse visibility. It was impractical to run all combinations of the factors shown in Fig. 5, so the combinations listed in Table 1 were selected to span the major dimensions, with emphasis on combinations likely to show degraded performance (i.e., higher speeds, shorter visibility ranges, and shorter delineation elements).

Typical examples of visibility and configuration conditions are illustrated in Figs. 6 and 7. In Fig. 6 it is apparent how reduced visual range affects lateral position, heading, and curvature cues. In Fig. 7 the effects

TABLE 1. SIMULATION EXPERIMENTAL CONDITIONS

VISIBILITY RANGE (ft)	SPEED (mph)	CONFIGURATION		CONFIGURATION VISIBILITY PARAMETER, C_V (Dimensionless)	PLOTTING SYMBOL[b]
		MARK/CYCLE LENGTH (ft)	LEFT/RIGHT LANE EDGE CONFIGURATION[a]		
300	30	15/40	D/D	0.09	▶
100	30	15/40	D/D	0.28	▼
100	55	15/40	D/D	0.28	▼
100	30	2/40	D/D	0.54	■
100	55	2/40	D/D	0.54	■
50	15	9/25	D/D	0.44	⊙
50	30	9/25	D/D	0.44	⬢
50	55	9/25	D/D	0.44	⬢
50	15	15/40	D/D	0.55	◁
50	30	15/40	D/D	0.55	◀
50	55	15/40	D/D	0.55	◀
50	15	2/40	D/D	1.08	◇
50	15	2/40	D/S	1.08	◇
50	15	2/40	D/N	1.08	◇
50	30	2/40	D/D	1.08	◆
50	30	2/40	D/N	1.08	◆
50	30	2/40	D/S	1.08	◆
35	15	15/40	D/D	0.79	△
35	30	15/40	D/D	0.79	▲

[a]D - dashed; S - solid; N - none.

Categorized as follows:
3-sided symbols used for 15/40 (MUTCD Standard)
6-sided symbols used for 9/25 (California Standard)
4-sided symbols used for 2/40 (MUTCD Standard cycle length with short marks or RPMs)

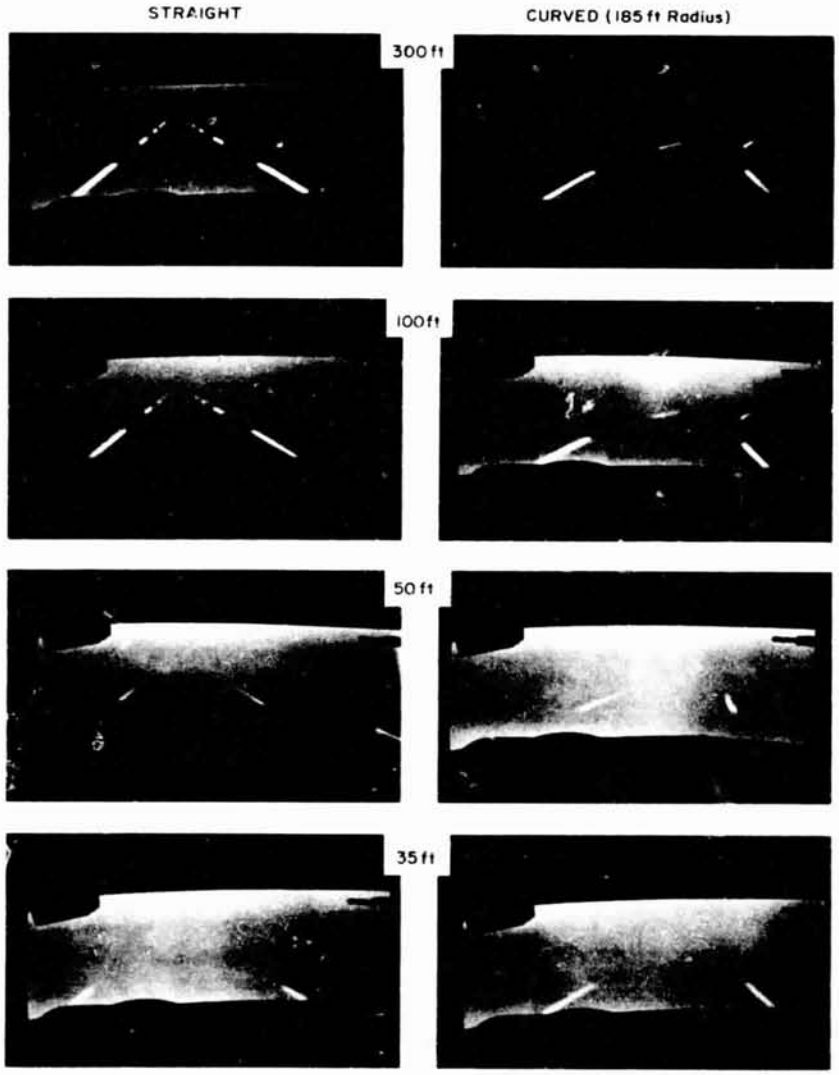

Figure 6. Federal Standard Delineation Striping Under Various Levels of Reduced Visibility

P-202

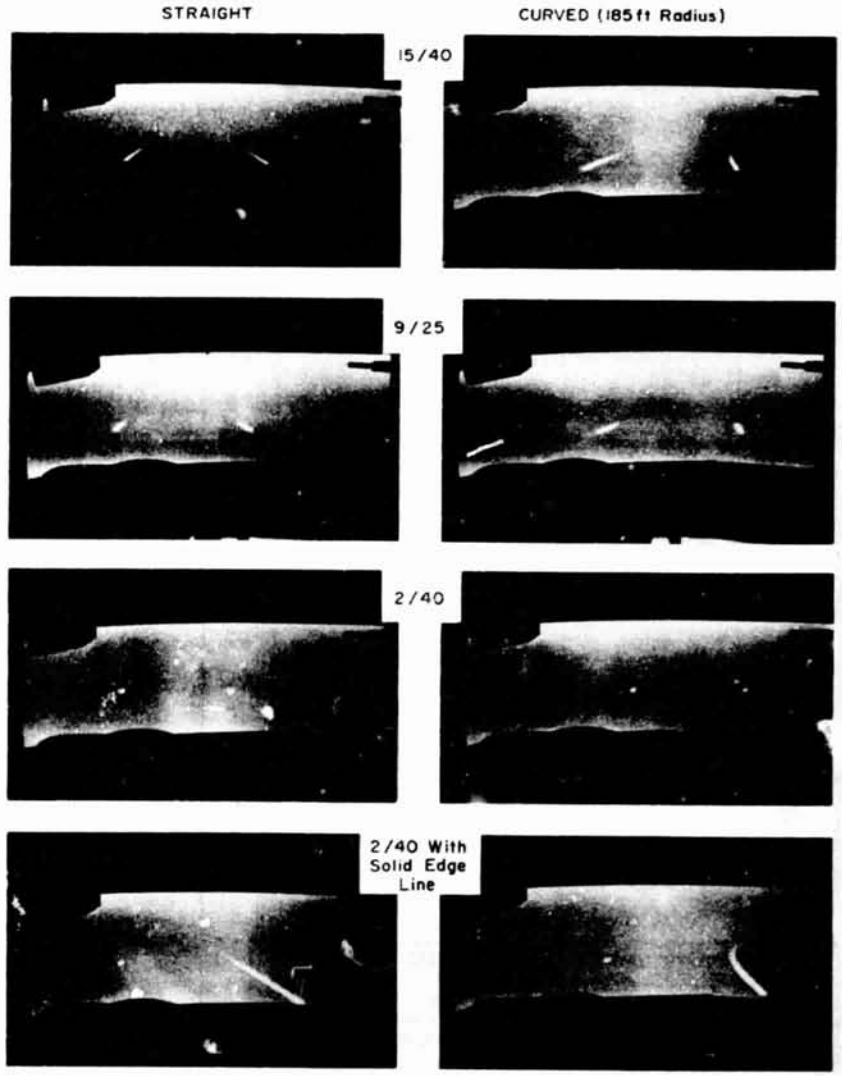

Figure 7. Delineation Configuration Variations Under 50 ft Visual Range

P-202

of the various delineation configurations under reduced visual range are apparent; the decreased directional cues with shorter delineation elements, and the vast improvement with a solid edge line.

Based on the exploratory experiment results a configuration visibility parameter listed in Table 1 was developed to quantify the combined perceptual effects of delineation configuration and visual range. As illustrated in Fig. 8, the configuration visibility parameter has two components. The first, $(x_g + x_o)/x_v$, is related to the number of delineation elements visible. For $(x_g + x_o)/x_v > 1$ we see from Fig. 8 that delineation elements close to the car are obscured by the hood before the next element becomes visible down the road (hood visibility obstruction in the simulator was 19 ft). The second

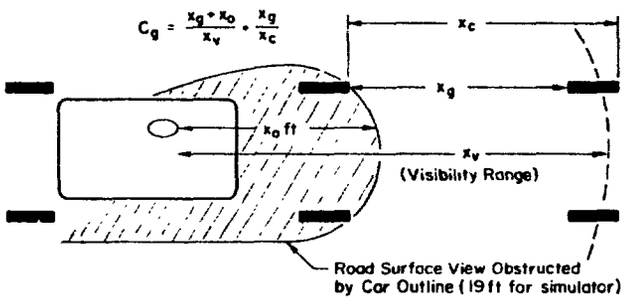

Figure 8. Configuration Visibility Parameter for Quantifying the Combined Effects of Delineation Configuration and Visual Range

factor, x_g/x_c, roughly quantifies the proportion of available information when delineation elements are visible. Thus, the configuration parameter gives large values for poor visibility, large gaps, and large proportions of gap-to-cycle length ratio, and driver performance would be expected to deteriorate under these conditions. The configuration parameter quantifies therefore both the visual segment and intermittency aspects of the driver's visual scene. This parameter thus far only accounts for symmetrical delineation, however, and we will have to consider the performance effects to determine what influence the right edge line variations will have.

Procedures

Six licensed drivers with normal vision were selected as test subjects. Background on the subjects is given in Table 2. Prior to the formal testing/data-gathering experiments, each subject was given a brief introductory session that consisted of driving the test scenario twice through each baseline configuration. The purpose of these sessions was twofold: 1) to transition subjects' skills of everyday automobile driving to the fixed-base simulator environment; and 2) to introduce the subject to the general nature of the test plan and procedures. These initial sessions were intentionally short in order to minimize training efforts and avoid overlearning.

TABLE 2. SUBJECT BACKGROUND

SUBJECT	SEX	AGE	DRIVING EXPERIENCE (IN YEARS)	EDUCATION
A	M	29	17	B.S.
B	M	21	5	A.A.
C	M	33	17	A.S.
D	M	29	13	A.A.
E	F	41	24	H.S.
F	F	17	1	H.S.

Typically, each subject drove the entire test scenario in two or three days of concentrated testing. Each day was broken into four test sessions of one to one and a half hours each separated by a rest period. At the beginning and end of each day, the 300 ft baseline configuration was tested. At the beginning and end of each session, a baseline configuration was administered, either the 300 ft or 50 ft visibility condition. Baseline conditions were also periodically interspersed within the sessions. All configurations in the experiment were given to the subjects in a pseudo-random order. At no time was a subject aware of what conditions would be driven next.

In order to control for within- and between-subject variations in contrast thresholds and equipment variations, visibility distance was individually set

for each condition according to the following procedure. The experimenter would initially set the visibility range, then ask the subject to position a line, which appeared across the roadway, to the point at which the delineation disappeared. The line position was controlled with a ten-turn potentiometer and was returned to zero between estimates. The experimenter would repeat this procedure several times, readjusting the visibility range between estimates in an iterative procedure until the desired visibility range, as indicated by the subject, was achieved.

Tasks and Measures

Describing function and performance measurements were obtained under two task conditions for each experimental condition. One task required regulating against a random wind gust-like disturbance added in at the steering signal input to the vehicle equations of motion as illustrated in Fig. 2. This task required compensatory control behavior as the roadway was straight and the disturbance could not be observed other than in its effect on vehicle motions. A second task involved following a winding road which allowed for pursuit control behavior if the visual scene provided for adequate curvature perception. Curvature commands for this task were added into the equations as shown in Fig. 2 in addition to curving the displayed roadway.

The method for obtaining driver describing function data is shown in Fig. 8. A Fourier analyzer (Ref. 19) generated a sum of sine waves input (Table 3) that was injected into the system as either a command or a disturbance, and received back another system quantity which was subsequently Fourier analyzed at each of the input frequencies ω_i.

As noted in Fig. 8 the actual quantities used to compute the equivalent driver/vehicle open-loop describing function depend on the task input. For the winding road command input case, where pursuit behavior is possible, the error (r_e) to input (r_c) describing function is computed and then transformed to give an equivalent open-loop transfer function r/r_e. For the compensatory, wind gust disturbance input the equivalent open-loop transfer function is found from operations on the δ_e/δ_d ratio, as described in Ref. 9.

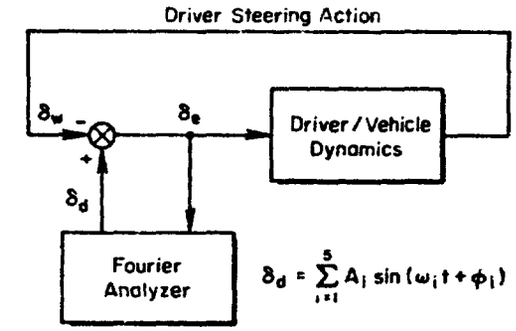

a) Wind Gust Disturbance Input

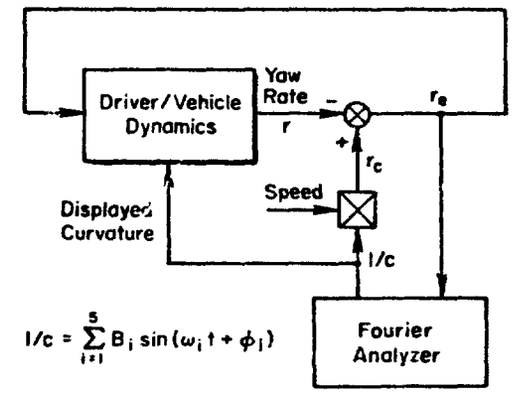

b) Winding Road Command Input

Figure 8. Driver Describing Function Measurement Technique

TABLE 3. INPUT AMPLITUDES AND FREQUENCIES

FREQUENCY (rad/sec)	WIND GUST AMPLITUDES (EQUIVALENT FRONT WHEEL ANGLE, deg)	ROAD CURVATURE AMPLITUDES (INVERSE RADIUS OF CURVATURE, ft^{-1})
0.188	0.172	2.07×10^{-3}
0.503	0.172	2.06×10^{-3}
1.25	0.172	1.98×10^{-3}
3.	0.172	1.66×10^{-3}
6.28	0.086	0.56×10^{-3}
rms	0.251	2.79×10^{-3}

After the describing function data are developed, an optimal identification routine is used to find driver parameters for the Fig. 2 system model that will give a good match to the measured describing function data.

As an example consider the data illustrated in Fig. 9 for the two baseline visibility conditions. The measured describing functions were averaged across six subjects, and the describing function fits match the data rather well. The characteristic effect of the curve perception parameter K_{R_C} is apparent in both cases in comparing the compensatory (wind gust disturbance) and pursuit (winding road command) tasks.

RESULTS

Model parameters for both steering tasks over a number of visibility and delineation configuration conditions are compared in Table 4. The most apparent consistent effect in the complete model parameters seems to be the reduction in curvature perception (K_{R_C}) with increased configuration visibility parameter C_V. This relationship is plotted in Fig. 10. Although the effects are not as neat as we might hope, the tendencies are quite clear: curve perception gain decreases with increasing configuration visibility parameter, and decreasing speed. Changes due to C_V are undoubtedly associated with the amount of curvature information provided by the visual segment on a

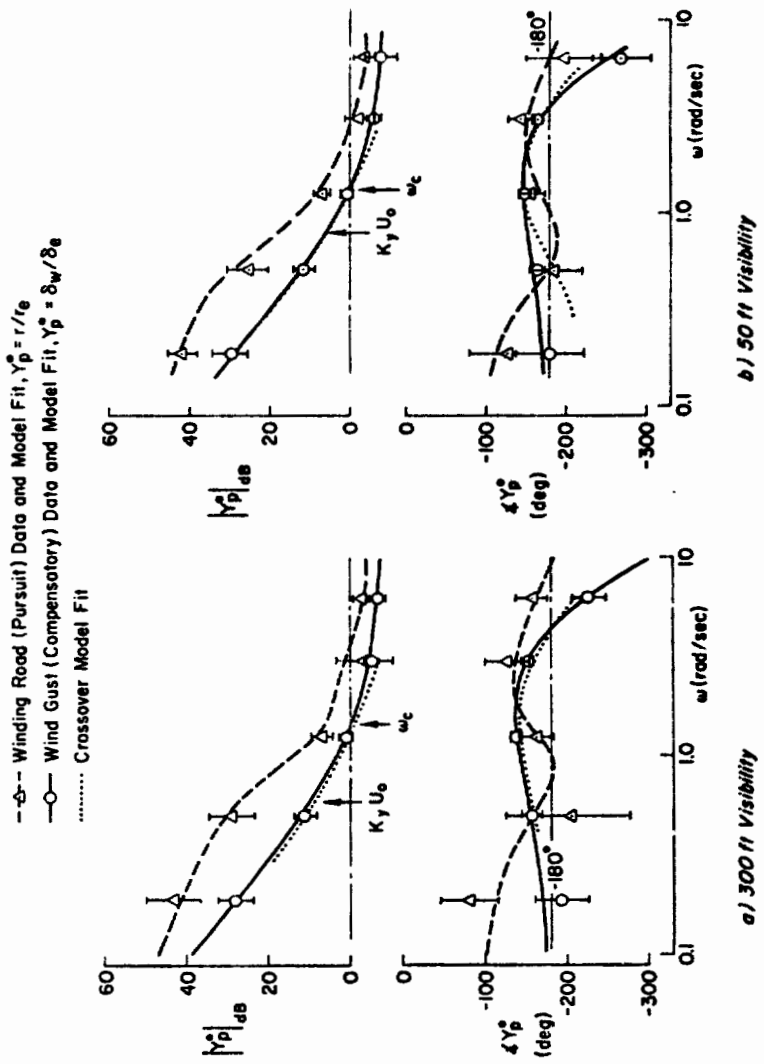

Figure 9. Baseline Condition Driver/Vehicle Describing Functions and Transfer Function Model Fits

TABLE 4. DYNAMIC RESPONSE PARAMETERS

EXPERIMENTAL CONDITION				PURSUIT (WINDING ROAD COMMAND)						COMPENSATORY (WIND GUST DISTURBANCE)							
				MODEL FIT PARAMETERS						COMPLETE MODEL FIT PARAMETERS						CROSSOVER CHARACTERISTICS	
VISIBILITY RANGE (ft)	MARK/CYCLE LENGTH (ft)	CONFIGURATION VISIBILITY PARAMETER, C_v	SPEED, U_o (mph)	$\frac{K_{R_c}}{\ell}$	K_y (ft^{-1})	K_v	T_L (sec)	τ (sec)		K_y (ft^{-1})	K_v	T_L (sec)	τ (sec)	$\frac{1}{K_y U_o}$ (sec)		ω_c (rad/sec)	ϕ_m
300	15/40	0.09	30	0.857	0.0587	0.174	0.247	0.422		0.022	0.195	0.471	0.520	1.03		1.46	39.0
100	2/40	0.54	30	0.903	0.0286	0.136	0.164	0.450		0.0355	0.105	0.652	0.600	0.64		1.15	28.23
50	9/25	0.44	15	0.795	0.159	0.220	0.276	0.490		0.0130	0.274	0.342	0.691	3.5		0.835	45.0
50	9/25	0.44	30	0.959	0.0114	0.260	0.152	0.551		0.0319	0.141	0.563	0.628	0.71		1.38	26.4
50	9/25	0.44	55	1.005	0.0098	0.224	0.154	0.377		0.0258	0.132	0.477	0.471	0.48		21	13.76
50	15/40	0.55	15	0.772	0.0436	0.156	0.310	0.518		0.0113	0.315	0.109	0.41	1.0		0.785	42.86
50	15/40	0.55	30	0.856	0.0218	0.244	0.241	0.540		0.0251	-0.169	0.483	0.600	0.9		1.30	27.38
50	15/40	0.55	55	0.979	0.0033	0.0769	0.769	0.604		0.0231	0.133	0.530	0.552	0.54		2.20	13.33
50	2/40	1.08	30	0.571	0.0819	0.0854	0.453	0.58		0.0301	0.154	0.389	0.652	0.76		1.12	16.9
35	15/40	0.79	15	0.141	0.0605	0.355	0.447	0.387		0.0116	0.223	0	0.328	3.92		0.687	28.38
35	15/40	0.79	30	0.825	0.0143	0.26	0.115	0.529		0.0176	0.206	0.332	0.672	1.29		1.36	24.64

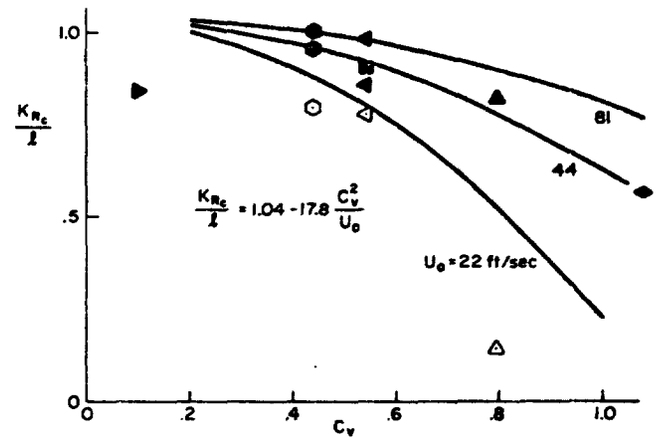

Figure 10. Effects of Adverse Visibility and Delineation Configuration on the Curvature Perception Parameter

static basis as discussed earlier. The speed effect is most likely related to the dynamic or "streaming" effect of delineation elements moving in the visual field, with higher speeds inducing a stronger perception of curvature.

Aside from the curve perception parameter, K_{RC}, the large number of parameters which comprise the complete model data in Table 4 exhibit covariations that make it difficult to focus the effects of adverse visibility on any one particular parameter. To permit more generalization we need a simpler summary of the driver's dynamic response that would nonetheless have properties pertinent to closed-loop driver/vehicle performance. For this purpose an "extended" crossover model is appropriate. For the equivalent compensatory open-loop transfer function of Fig. 11 this has the form:

$$\frac{\delta}{\delta_e} = \frac{s + (1/U_o K_y)}{s^2} \omega_c e^{-\tau_e s} \qquad (2)$$

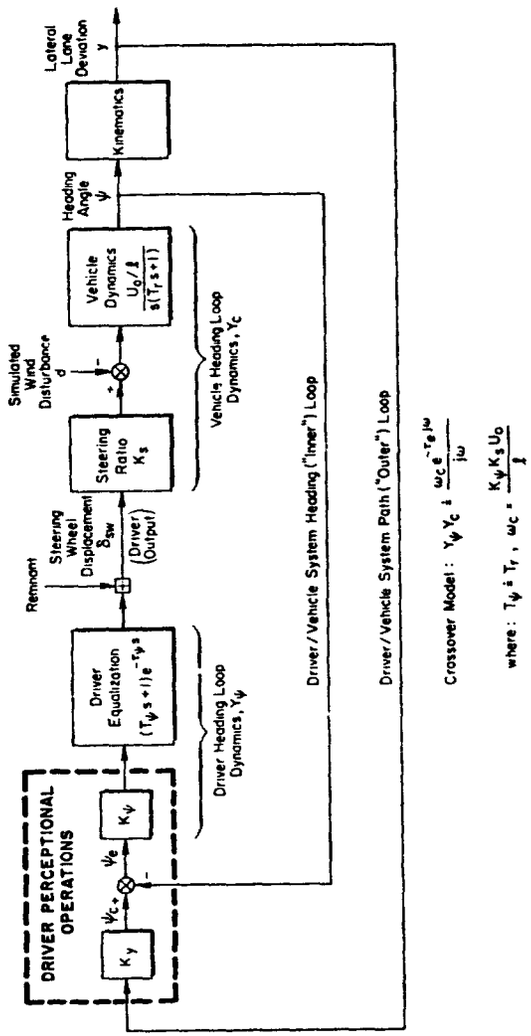

Crossover Model: $Y_\psi Y_c \doteq \frac{\omega_c e^{-\tau_e j\omega}}{j\omega}$

where: $T_\psi \doteq T_r$, $\omega_c = \frac{K_\psi K_s U_o}{\ell}$

Figure 11. Simplified Crossover Model Interpretation of Driver/Vehicle Steering Control

This relationship is based on the equivalent driver/vehicle transfer function developed in Ref. 9. The equivalent time delay τ_e combines the high-frequency phase properties of the driver (lead, neuromuscular lags, transport delay) and vehicle (basically the heading response dynamics). The crossover frequency, ω_c, combines the driver and vehicle heading gains which can be expressed by the useful approximation (Ref. 2)

$$\omega_c = \frac{K_\psi K_s U_o}{\ell} \tag{3}$$

where K_ψ is the driver's heading gain from the complete model, K_s is the steering ratio (which has arbitrarily been set to unity for all the K_ψ parameters reported herein), and ℓ is the vehicle wheelbase. The free s in the denominator of Eq. 2 approximates the wheel input to car heading angle dynamics. The phase lags of the additional high-frequency lag properties are accounted for in τ_e, and typical crossover frequencies are low enough that the high frequency amplitude properties are not important. Finally, the numerator zero at $(U_o K_y)^{-1}$ accounts for the driver's operations on lane position. $U_o K_y$ can be interpreted as an equivalent look-ahead time constant (T_a in Eq. 1) and K_y^{-1} is the corresponding look-ahead distance.

A simple approximation can be used to compute the parameters of Eq. 2. From moderately low to high frequencies, the phase angle of the numerator zero at $(U_o K_y)^{-1}$ can be approximated by an exponential (Ref. 20)

$$\measuredangle \frac{[s + (U_o K_y)^{-1}]}{s} \doteq e^{-\alpha/s} \tag{4}$$

where $\alpha = (U_o K_y)^{-1}$. Using this approximation, the phase of Eq. 2 then can be written as

$$\measuredangle \frac{\delta}{\delta_e} = -\tau_e \omega - \frac{\alpha}{\omega} - \frac{\pi}{2} \tag{5}$$

This equation can now be evaluated at the gain and phase crossover frequencies of the driver/vehicle describing function in order to solve for τ_e and α. At gain crossover frequency the phase angle is equal to π less the phase margin

φ_m, and the phase crossover is defined as the frequency at which the phase angle is equal to π. Therefore, τ_e and α can be computed from the equation:

$$\begin{bmatrix} \omega_c & 1/\omega_c \\ \omega_u & 1/\omega_u \end{bmatrix} \begin{bmatrix} \tau_e \\ \alpha \end{bmatrix} = \begin{bmatrix} (\pi/2) - \varphi_m \\ \pi/2 \end{bmatrix} \tag{6}$$

Using this relationship a few key dynamic response parameters can be calculated for the driver/vehicle system that are appropriate to the basic closed-loop properties and performance.

Cross-model parameters were fitted to all the wind gust disturbance (compensatory) conditions according to the above procedures, and these are listed in Table 5. The fits are representative of the data as illustrated in Fig. 9. Crossover modal parameters are plotted in Fig. 12. Heading gain, K_ψ, was computed from ω_c data using Eq. 3. There is a small effect of both configuration visibility and speed on K_ψ.

Inverse outer-loop (lane position) gain can be interpreted as an equivalent dynamic look-ahead distance and was computed using the relationship

$$K_y^{-1} \doteq U_o\alpha \tag{7}$$

The Fig. 11b plot of these data shows a strong dependence on C_V, with shorter distances apparently associated with restricted visual range (i.e., higher C_V values). There is little apparent speed dependence, however, suggesting that look-ahead distance is a more pertinent perceptual variable than the look-ahead time constant of Eq. 1.

Effective time delay, τ_e, is affected by both speed and configuration visibility parameter C_V. The increase in effective time delay with increase in C_V suggests that perceptual load associated with equalization and extrapolation increases with the reduction in the visual segment. Past research has postulated that τ_e increases are associated with an increase in driver lead equalization requirements and/or with the presentation of sampled information. In this case driver lead is used to offset the vehicle lag. But,

TABLE 5. EXTENDED CROSSOVER MODEL PARAMETERS

EXPERIMENTAL CONDITION				ω_c (rad/sec)	ω_u	φ_m	τ_e (sec)	$\alpha \doteq U_oK_y$ (rad/sec)	$\frac{1}{U_oK_y}$ (sec)	K_y^{-1} (ft)	K_ψ
VISIBILITY RANGE (ft)	MARK/CYCLE LENGTH (ft)	CONFIGURATION VISIBILITY PARAMETER, C_V	SPEED, U_o (mph)								
300	15/40	0.09	30	1.462	4.290	39.02	0.334	0.587	1.70	75	0.307
100	15/40	0.28	30	1.295	3.758	35.56	0.375	0.601	1.66	73.2	0.272
100	15/40	0.28	55	2.167	4.385	22.48	0.298	1.153	0.867	70	0.249
100	2/40	0.54	30	1.147	3.672	28.23	0.372	0.747	1.34	59	0.241
100	2/40	0.54	55	2.060	3.800	13.76	0.317	1.398	0.715	58	0.237
50	5/25	0.44	15	0.835	3.367	45.02	0.436	0.352	2.84	62	0.351
50	9/25	0.44	30	1.377	3.528	26.44	0.381	0.806	1.24	55	0.289
50	9/25	0.44	55	2.21	3.565	13.96	0.341	1.269	0.788	64	0.254
50	15/40	0.55	15	0.785	3.312	42.86	0.440	0.375	2.67	59	0.330
50	15/40	0.55	30	1.302	3.607	27.58	0.375	0.782	1.23	56	0.274
50	15/40	0.55	55	2.205	3.299	13.33	0.371	1.146	0.87	70	0.253
50	2/40	1.08	15	0.595	2.687	24.78	0.516	0.495	2.02	44	0.250
50*	2/40	1.08	15	0.762	3.240	37.71	0.443	0.438	2.28	50	0.320
50*	2/40	1.08	15	0.643	3.395	26.2	0.416	0.544	1.84	40	0.270
50	2/40	1.08	30	1.117	2.895	16.29	0.436	0.893	1.12	49	0.235
50*	2/40	1.08	30	1.347	3.210	15.44	0.388	1.05	0.952	42	0.285
50*	2/40	1.08	30	1.253	3.705	26.70	0.365	0.812	1.23	54	0.263
35	15/40	0.79	15	0.687	2.918	28.38	0.478	0.516	1.93	43	0.289
35	15/40	0.79	30	1.355	2.897	24.64	0.458	0.704	1.42	62	0.285

*Not used in regression analysis because of non-symmetrical delineation (see Table 1).

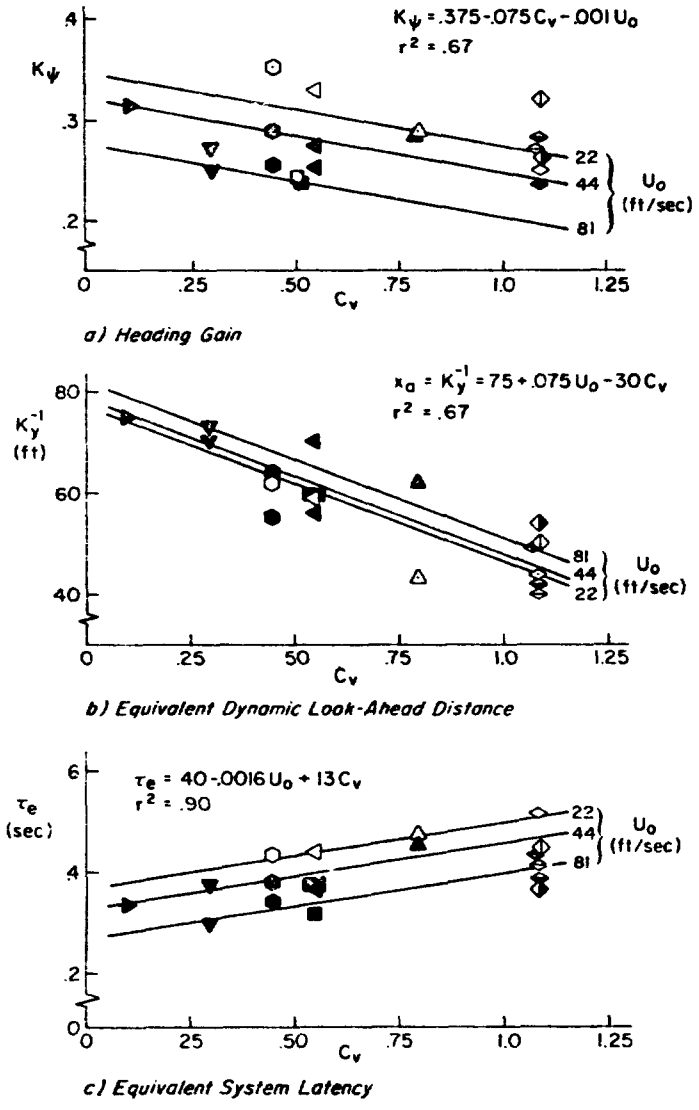

Figure 12. Driver/Vehicle System Extended Crossover Model Parameters for Compensatory Task

the vehicle lag increases with speed whereas the effective time delay decreases with speed, so this "explanation" is in the wrong direction. The sampling interval of the dashed lines is given by

$$T_s = \frac{x_c}{U_o} \tag{8}$$

where x_c is the delineation cycle length. Change in τ_e is proportional to sampling interval (Ref. 15), so the variation of τ_e with both speed and C_v is in the right direction. Accordingly, we attribute the τ_e changes primarily to sampling processes associated with the delineation dashed lines and speed.

The sampling process which affects the driver's time delay should also have some influence on the noise or stochastic component of his steering actions. In Fig. 13 we show the proportion of noise or remnant that is uncorrelated with the driver's actions in counteracting wind gusts or steering along a winding road. There is a tendency for driver noise to increase both with configuration parameter and speed.

The intermittency of delineation apparently affects driver remnant; however, this effect is increased at higher speeds (i.e., higher delineation sample rates) in contrast to the time delay penalty (Fig. 12) which decreased with increasing speed. These two contrasting effects on driver behavior explain the relatively consistent effect of speed on performance under adverse visibility shown in Fig. 14. At low speeds, the slow intermittency of delineation causes appreciable increases in driver time delay which degrades performance; while at high speeds, driver noise increases, which again degrades performance. Also note that for the curve-following data driver noise increases appreciably under the same conditions that led to reduced curvature perception (Fig. 10). Furthermore, the curve-following data show a proportionately greater configuration visibility parameter sensitivity, consistent with the Fig. 14 performance data. A final observation is that the solid edge line reduces driver noise over the dashed or no right lane line cases, which (as with previously discussed data) is consistent with a lower equivalent C_v.

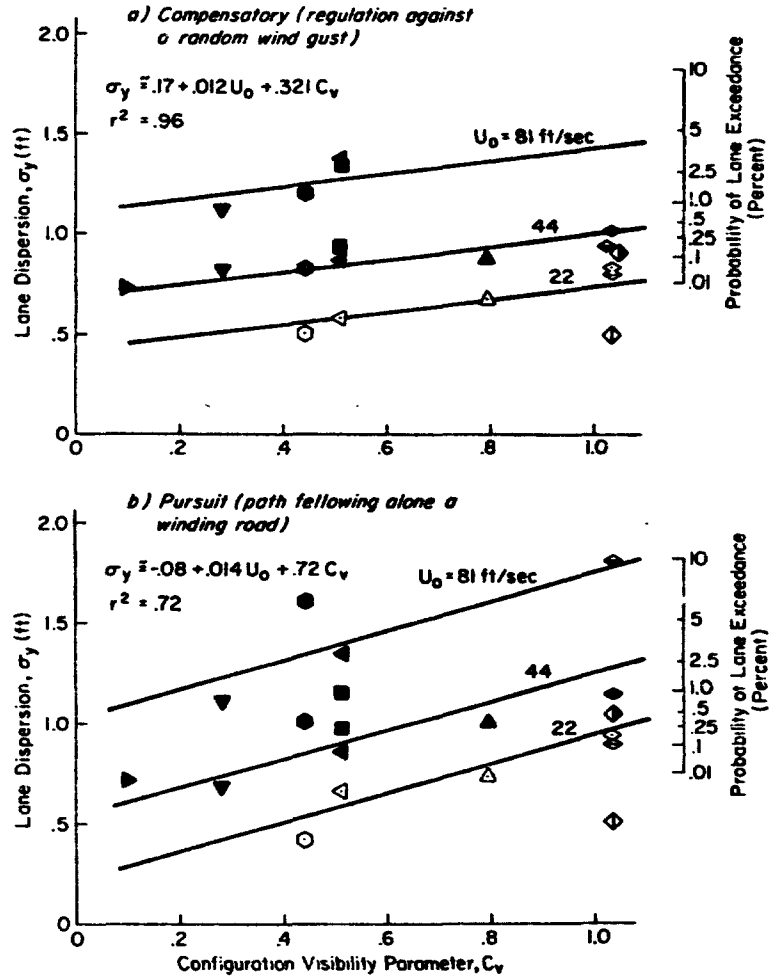

Figure 14. Lane Dispersions as a Function of Speed and Configuration Visibility Parameter

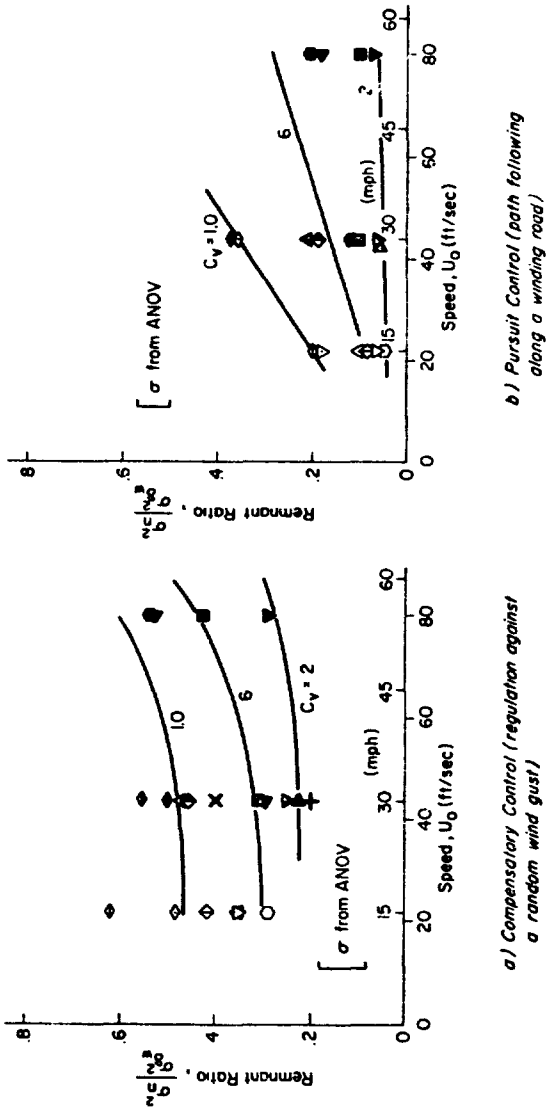

Figure 13. Driver Remnant as a Function of Speed and Configuration Visibility Parameter

CONCLUDING REMARKS

Adverse visibility restricts the driver's perception of automobile path and motion information required for steering control. These perceptual restrictions can be quantified in terms of the driver's dynamic steering behavior in response t random disturbances and path commands. Combinations of reduced visibility and delineation configuration (i.e., intermittent dashed or dotted lines) tend to induce increased transport delay in the driver and impair his perception of road curvature. Reduced visibility also induces a reduction in equivalent dynamic look-ahead distance (the inverse of lateral position error gain) but does not appear to influence the weighting or gain the driver applies to heading errors.

The above effects appear to be related to the apparent intermittent or sampled nature of delineation under reduced visibility conditions. Driver time delay, τ_e, increases at slower speeds, due to decreased sampling frequency, even though vehicle dynamic lags decrease with speed. This effect induced a somewhat compelling urge in some subjects to speed up in order to increase their information rate, which is a rather insidious phenomenon if true for real-world driving, since it might encourage drivers to maintain speeds with associated stopping distances exceeding their visual range.

Changes in curve perception gain also appear to be related to information sampling, with KR_C decreasing with decreased speed and/or reduction in the amount of perceptual information (i.e., increased C_V). In this case curvature perception is enhanced with speed, which may also be related to "streamer" theories of driver perception where the curved path motion of the car is indicated by the curved motion of visual field elements.

This research has given some insight into dynamics of driver perception, and the role played by road markings used to delineate the commanded pathway. The techniques developed here should be ı ıl for further research in this area and allow various questions to be an ered about the required or optimal configurations of roadway delineation.

REFERENCES

1. Segel, L., "Theoretical Prediction and Experimental Substantiation of the Response of the Automobile to Steering Control," in Research in Automobile Stability and Control and in Tyre Performance, London, Institute of Mechanical Engineers, 1957.

2. Allen, R. W., and D. T. McRuer, "The Effect of Adverse Visibility on Driver Steering Performance in an Automobile Simulator," presented at the 1977 SAE International Automobile Engineering Congress and Exposition, Detroit, 28 Feb.-4 Mar. 1977.

3. Gibson, J. J., "What Gives Rise to the Perception of Motion," Psych. Review, Vol. 75, 1968, pp. 335-346.

4. Gordon, D. A., "Perceptual Basis of Vehicular Guidance," Public Roads, Vol. 34, No. 3, Aug. 1966, pp. 53-68.

5. Palmer, E. A., "Experimental Determination of Human Ability to Perceive Aircraft Aimpoint from Expanding Gradient Cues," Aerospace Medical Meeting, San Francisco, Preprint of Scientific Program, May 1969, pp. 176-177.

6. Calvert, E. S., "Visual Judgments in Motion," J. Inst. Navigation, Vol. 7, 1957.

7. Haines, R. F., "A Review of Peripheral Vision Capabilities for Display Layout Designers," Proc. S.I.D., Vol. 16/4, Fourth Quarter, 1975, pp. 238-249.

8. McRuer, D. T., R. W. Allen, D. H. Weir, and R. H. Klein, "New Results in Driver Steering Control Models," Human Factors, Special Issue, forthcoming.

9. McRuer, D. T., D. H. Weir, H. R. Jex, R. E. Magdaleno, and R. W. Allen, "Measurement of Driver/Vehicle Multiloop Response Properties with a Single Disturbance Input," IEEE Trans., Vol. SMC-5, No. 5, Sept. 1975, pp. 490-497.

10. McLean, J. R., and E. R. Hoffmann, "The Effects of Restricted Preview on Driver Steering Control and Performance," Human Factors, Vol. 15, No. 4, Aug. 1973, pp. 421-430.

11. Weir, D. H., and D. T. McRuer, "Dynamics of Driver/Vehicle Steering Control," Automatica, Vol. 6, No. 1, Jan. 1970, pp. 87-98.

12. McRuer, D. T., R. H. Klein, et al., Automobile Controllability — Driver/Vehicle Response for Steering Control. Vol. I: Summary Report. Vol. II: Supporting Experimental Results, DOT HS-801 407 and HS-801 406, Feb. 1975.

13. McRuer, D. T., "Simplified Automobile Steering Dynamics for Driver Control," presented to the SAE Aerospace Control and Guidance Systems Comm. Mtg. No. 35, Palo Alto, Calif., 19-21 Mar. 1975.

14. McRuer, D. T., and E. S. Krendel, Mathematical Models of Human Pilot Behavior, AGARD-AG-188, Jan. 1974.

15. Allen, R. W., W. F. Clement, and H. R. Jex, Research on Display Scanning, Sampling, and Reconstruction Using Separate Main and Secondary Tracking Tasks, NASA CR-1569, July 1970.

16. Allen, R. W., J. R. Hogge, and S. H. Schwartz, "A Simulator for Research in Driver, Vehicle and Environment Interaction," presented at the 56th Meeting of the TRB, Jan. 1977.

17. Traffic Manual, State of California, Business and Transportation Agency, Dept. of Public Works, 1971.

18. Manual on Uniform Traffic Control Devices for Streets and Highways, Federal Highway Admin., 1971.

19. Allen, R. W., and H. R. Jex, "A Simple Fourier Analysis Technique for Measuring the Dynamic Response of Manual Control Systems," IEEE Trans., Vol. SMC-2, No. 5, No. 1972, pp. 638-643.

20. McRuer, D., D. Graham, E. Krendel, and W. Reisener, Jr., Human Pilot Dynamics in Compensatory Systems — Theory, Models, and Experiments with Controlled Element and Forcing Function Variables, AFFDL-TR-75-15, July 1965.

ACKNOWLEDGMENT

This work was supported by the Federal Highway Administration under Contract DOT-FH-11-8824. Dr. Donald A. Gordon of the Traffic Systems Division served as the Contract Technical Manager.